

H-mode transition and E_r formation analysis of NSTX based on the gyrocenter shift

K. C. Lee 1), R. Bell 2), C. W. Domier 1), B. P. LeBlanc 2), S. A. Sabbagh 3),
H. K. Park 4), N. C. Luhmann, Jr. 1), R. Kaita 2) and NSTX research team

1) Department of Applied Science, University of California, Davis, California 95616, USA

2) Princeton Plasma Physics Laboratory, Princeton, New Jersey 08543, USA

3) Columbia University, New York, New York 10027, USA

4) POSTECH, Pohang, Kyungbuk 790-784, Korea

E-mail contact of main author: kclee@pppl.gov

Abstract: The radial current generated by the ion-neutral momentum exchange has been analyzed to be responsible for the radial electric field (E_r), the turbulence transport, and the low confinement mode (L-mode) to high confinement mode (H-mode) transitions on the edge of tokamak plasmas. In this analysis of gyrocenter shift the plasma pressure gradient, the neutral density gradient and the neutral velocity are the major driving mechanism of the radial current and the electric field is formed as the source of the return current to make an equilibrium condition. When there is turbulence the small scale ExB eddies induce the cross-field transport. Finally the origin of turbulence is interpreted that it comes from the friction between the plasma and the neutrals so that the Reynolds number determines the state between laminar flow (H-mode) and turbulent flow (L-mode). The confinement time of the national spherical torus experiment (NSTX) is compared with the density fluctuation level to verify the turbulence induced diffusion coefficient from the theory of gyrocenter shift. The calculation results based on the gyrocenter shift for the poloidal velocity of carbon impurity ions are compared with CHERS measurement of NSTX plasmas. The calculation result agreed within 50% discrepancy which is closer than the results from neoclassical simulation codes.

1. Introduction

One of the crucial obstacles of the nuclear fusion energy development is that the experimental cross-field particle transport is hundreds of times larger than the expected by the classical diffusion theory. As a result of the effort to overcome this anomalous transport the low confinement to high confinement mode transition (L/H transition) was experimentally discovered [1]. After decades of study of the L/H transition mechanism, the following gyrocenter shift current (comes from $\mathbf{J} \times \mathbf{B}$ as momentum exchange of the ion-neutral collisions) is suggested as the origin of the radial electric field which is regarded as the triggering parameter of L/H transition [2,3].

$$J^{GCS} = en_i \frac{r_{Li}}{\lambda_{cx}} \left[\frac{E}{B} - \frac{\nabla P_i}{eBn_i} - v_n + \frac{kT_i \nabla n_n}{eBn_n} \right] \quad (1),$$

where e is ion charge, n_i is ion density, r_{Li} is ion gyro-radius, λ_{cx} is ion mean free path of charge exchange with neutrals, E is electric field, B is magnetic field, P_i is ion pressure, kT_i is ion thermal energy, v_n is neutral velocity and n_n is neutral density. The four terms in the bracket of Eq.(1) compose the effective velocity (v^*), which is illustrated in Fig.1.

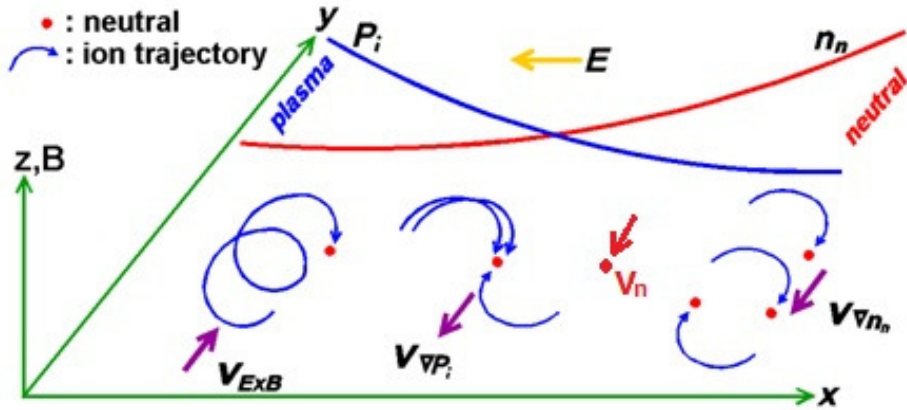


Fig.1 Four components of ion velocity that make momentum exchange (v^*); v_{ExB} is ion ExB drift, $v_{\nabla P_i}$ is ion diamagnetic drift, v_n is neutral velocity and $v_{\nabla n_n}$ is the component of the effective ion velocity induced by the neutral density gradient.

Three terms of $v_{\nabla P_i}$, v_n , and $v_{\nabla n_n}$ are the driving mechanism of J^{GCS} and E_r is formed as the source of the return current to compensate driving terms. When there is turbulence the small scale ExB eddies induce the cross-field transport and the equilibrium condition is set with a smaller radial electric field than without turbulence case since ExB eddies also generate additional return currents. The cross-field transport induced by the turbulence eddies is described by the diffusion coefficient which is responsible for the turbulence induced anomalous transport [4].

In section 2, two experimental results from NSTX are discussed based on the gyrocenter shift, and the analysis of the core radial electric field formation is introduced in section 3 followed by the conclusion.

2. Density fluctuation level vs. EFIT confinement time

The confinement time from the EFIT equilibrium [5] of the national spherical torus experiment (NSTX) is compared with the density fluctuation level measured by the far infrared tangential interferometry/polarimetry (FIRETIP) [6] to verify the turbulence induced diffusion coefficient (D) from the theory, which is illustrated in Fig.2 (a) and (b). According to the Ref. 4, the turbulence diffusion coefficient can be described as following,

$$D = \frac{2}{\pi} \eta \left(\eta + \frac{\lambda_i}{2L_n} \right) \frac{kT_i}{eB} \quad (2),$$

where, D is the diffusion coefficient, η is the density fluctuation level, λ_i is the turbulence wave length, and L_n is the neutral density scale length. To verify this, the measured density fluctuation level is compared with the confinement time. The chord –averaged density fluctuation is measured by the multichannel FIRETIP system using the most effective channel (CH5) whose beam path includes the separatrix region. The EFIT confinement time is plotted as function of density fluctuation level on the basis that the confinement time is inversely proportional to the diffusion coefficient.

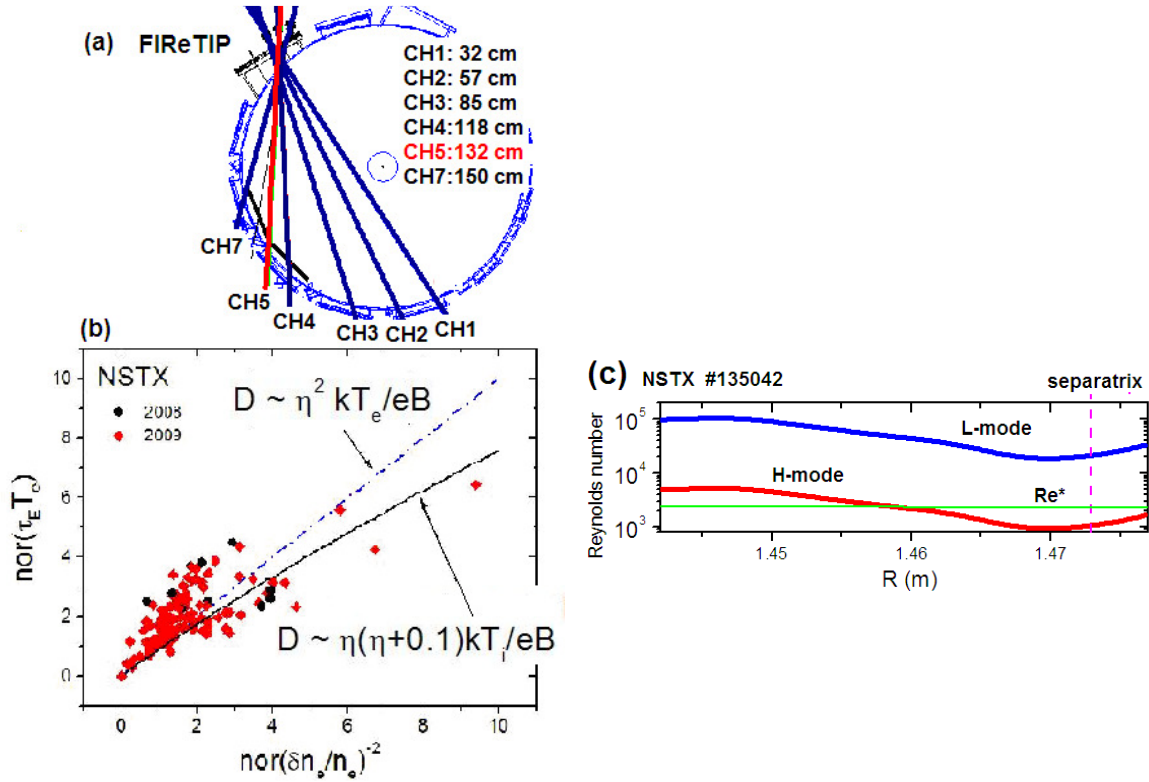


Fig.2 Experimental measurement of NSTX plasmas for the comparison with gyrocenter shift theory, η is density fluctuation level.

At least two time points are selected for each plasma shot avoiding Magnetohydrodynamic (MHD) activities such as Edge Localized Modes (ELMs), and both confinement time and density fluctuation level are normalized by the value of first point. Every point in the graph which has two parameters, $(\text{nor}(\frac{\delta n_e}{n_e})^{-2}, \text{nor}(\tau_E T_e))$ comes from two points in time of same

shot. For example of $(\frac{\delta n_e}{n_e})^{-2}$, normalization means that $\text{nor}(\frac{\delta n_e}{n_e})^{-2}$ is $(\frac{\delta n_e}{n_e})^{-2}$ of that point

divided by $(\frac{\delta n_e}{n_e})^{-2}$ of first point. In this way most of the influences from other plasma

conditions are eliminated. Since the diffusion coefficient of Eq.(2) is a function of temperature, the temperature inside the separatrix is included in the plots. Equation (2) is induced by using a modified Boltzmann relation which includes the neutral density gradient in the force balance. Figure 2 shows that the measurement is a close fit to the turbulent diffusion coefficient derived from the gyrocenter shift.

One of the important results in the Ref. 4 is that the ion-neutral collisions include the inertia force and the friction force so that their ratio can be defined as Reynolds number which is described by the following,

$$\text{Re} \equiv \frac{n_i m_i v^{*2} / r_{Li}}{n_i m_i v_{cx} v^*} = \frac{\lambda_{cx} v^*}{r_{Li} v_{th}^i} \quad (3),$$

where m_i is ion mass, v_{cx} is the charge exchange reaction rate, v^* is the effective velocity and v_{th}^i is the ion thermal velocity. When there is higher intensity turbulence the magnitude of E becomes smaller and so does v_{ExB} then v^* becomes larger (since v^* is the difference between v_{ExB} and the summation of other three terms in Eq.(1)). This relation of Reynolds number explains two important characteristics of the L/H transition. First, the Reynolds number is proportional to the magnitude of turbulence itself therefore when the Reynolds number of a turbulent plasma reaches down to the critical value not only it just turns into the laminar state (H-mode) but also makes more reduction of Reynolds number so that the hysteresis is generated. Second, it explains the sudden increase of the radial electric field at the moment of the L/H transition because the reduction of turbulence require more of return current from the electric field to make a new equilibrium condition. A calculation of the Reynolds number from various measurements on NSTX plasma is shown in Fig.2 (c). When the plasma is L-mode Reynolds numbers are above the critical value (~ 2300) and when it becomes H-mode the Reynolds numbers are below the critical value around the region where the edge transport barrier forms.

3. E_r formation by Neutral Beam Injection

As indicated in Fig.1 and Eq.(1), when there is one directional movement in neutrals at the ion-neutral collisions the perpendicular component of v_n generates radial current. Since the neutrals of Neutral Beam Injection (NBI) have high energy (up to 90 keV) small number of ion-neutral collisions can transfer large amount of momentum to the ions. As shown in Fig.3, beam neutral's velocity has no poloidal component, and the possible contribution by radial component of the beam neutrals to the poloidal current is not included here since it is not related with radial electric field. The momentum transfer from beam neutrals to the main ions can be analysed by separating it into parallel and perpendicular components. Each component satisfies the momentum conservation respectively. For parallel momentum transfer, total momentum gain from beam neutrals during the time period of τ is;

$$N_i^t m_i v_{||}^i = \int_0^\tau N_i^b m_i \sigma v_r n_{NB} v_{NB} \cos \alpha dt$$
, where N_i^t is total number of ions that received momentum, $v_{||}^i$ is ion velocity in parallel direction, N_i^b is the number of ions that collide with beam neutral, σ is collision cross section, v_r is relative velocity of ion-neutral at the collision, n_{NB} is beam neutral density, and v_{NB} is the velocity of beam neutral. So $v_{||}^i \approx \tau (N_i^b / N_i^t) \sigma v_r n_{NB} v_{NB} \cos \alpha$. The perpendicular component of momentum transfer from beam neutrals to main ions contributes as radial current which is described in Eq.(1) and this radial current generates radial electric field, finally ions get velocity of ExB drift in perpendicular direction. So the perpendicular momentum gain of ions is;

$$N_i^t m_i v_{ExB} = \int_0^\tau N_i^b m_i \sigma v_r n_{NB} v_{NB} \sin \alpha dt$$
, and $v_{ExB} \approx \tau (N_i^b / N_i^t) \sigma v_r n_{NB} v_{NB} \sin \alpha$. So $v_{ExB} / v_{||}^i = \tan \alpha$. The parallel ($v_{||}^i$) and perpendicular (v_{ExB}) components of ion velocity increase in time. Obviously E_r is not in the same equilibrium condition of $v^* \approx 0$ as discussed in reference 4 and the measured E_r is in the range too much below to match the condition of $v_{ExB} \approx v_{NB}$ (note the disconnections in Fig.3 to indicate $v_{ExB} \ll v_{NB}$).

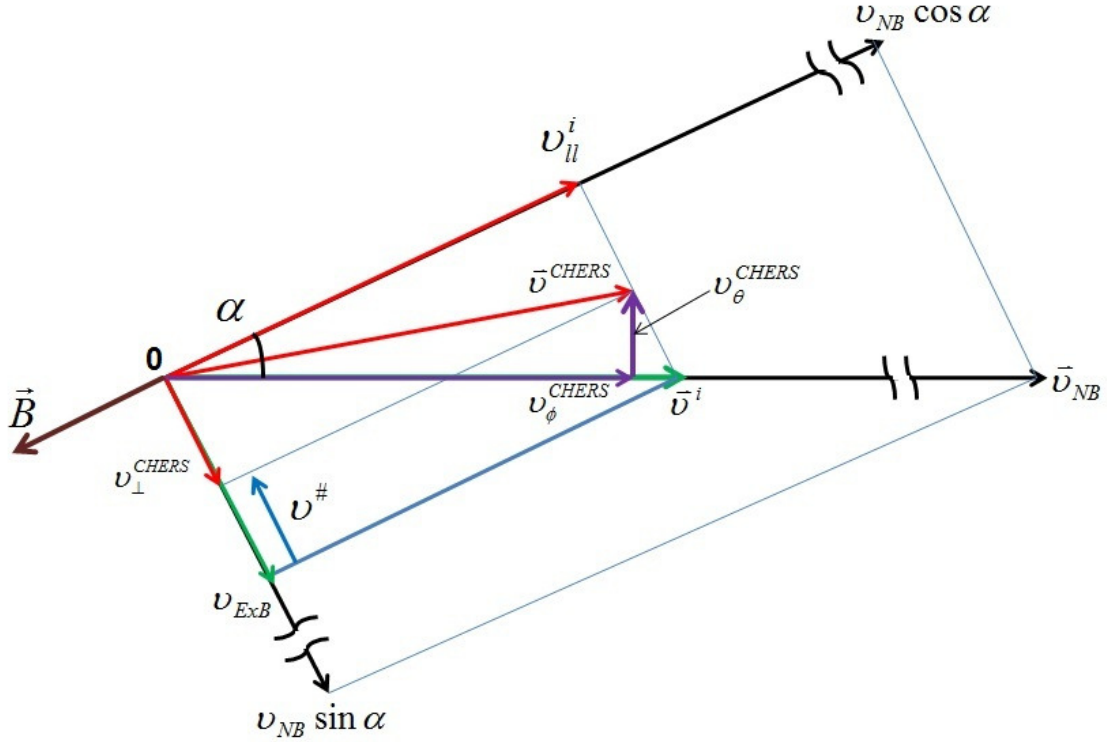


Fig.3 Schematic diagram of the E_r formation by neutral beam injection. Here horizontal direction is toroidal, vertical direction is poloidal, and α is pitch angle. The radial component of beam neutral velocity (v_{NB}) is not included in this diagram. The scale is exaggerated for the poloidal velocity measured by CHERS.

It is hard to tell the magnitude of ion velocity and E_r from above analysis, however the direction of ion velocity is clearly close to the pure toroidal as indicated in Fig.3 (the green arrow of \bar{v}^i). According to this analysis ion velocity measurement shouldn't show much of poloidal component. Recently Charge Exchange Recombination Spectroscopy (CHERS) of NSTX measured poloidal velocity and compared to the neoclassical theory [7]. CHERS measurement of ion velocity, under the assumption that carbon ions follow main ion velocity, has other perpendicular terms indicated as $v^\#$ in Fig.3. One is ion diamagnetic drift from the conventional force balance equation which is also indicated as $v_{\nabla P_i}$ in Fig.1. There is another term in $v^\#$ even bigger than $v_{\nabla P_i}$ which is induced by the asymmetric distribution of v_r around the circle of ion gyro-motion. The probability of collision is proportional to the relative velocity between ion and neutral, since v_r at left side is bigger than v_r at right side in Fig.4 (a), more ions in upward direction make collisions than ions with down direction. The net velocity induced by this asymmetry can be calculated by the average value over the circle indicated in Fig.4(a);

$$\int_0^{2\pi} \bar{v}_{th}^i v_r d\theta / \int_0^{2\pi} v_r d\theta \approx \frac{v_{th}^i{}^2}{2(v_{NB}^\perp - v_{th}^i)}, \quad \text{when } v_{th}^i/v_{NB} \ll 1, \quad \text{where } v_{NB}^\perp = v_{NB} \sin \alpha. \quad \text{The}$$

calculated values of v_θ^{CHERS} and the experimental measurement are compared in Fig.4 (b). The linear fit of calculation value is approximately within 50% of measured values in magnitude, which is better agreement than neoclassical simulations [7].

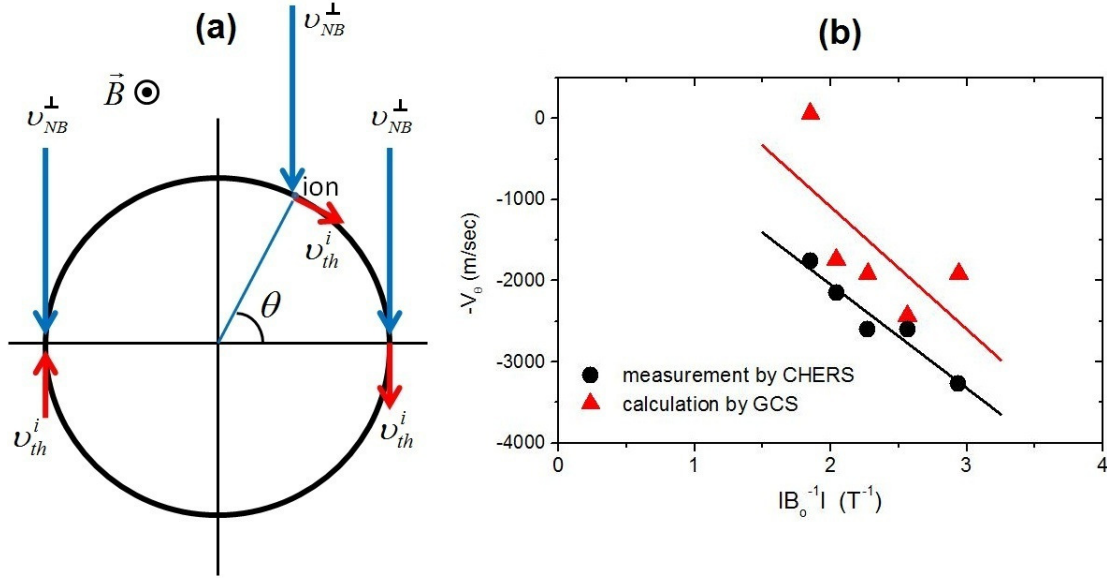


Fig.4 (a) Asymmetric distribution of relative velocity ($v_r = |\bar{v}_{th}^i - \bar{v}_{NB}^\perp|$, where $\bar{v}_{th}^i = -v_{th}^i \cos \theta \cdot \hat{y} + v_{th}^i \sin \theta \cdot \hat{x}$ and $\bar{v}_{NB}^\perp = -v_{NB}^\perp \cdot \hat{y}$) between ion and neutral that generates net perpendicular velocity term. v_r at left side is bigger than v_r at right side. (b) comparison of poloidal velocity of calculated from gyrocenter shift with the experimental measurement of CHERS for different poloidal magnetic fields. The data points were taken for the average of radius range from 137cm to 141 cm.

4. conclusion

The comparison of gyrocenter shift theory results for the experimental measurement of NSTX plasmas suggests that the gyrocenter shift is a reliable analysis for H-mode transitions and radial electric field formation. The gyrocenter shift should be included in the theory and simulations for the systematic research on the tokamak turbulence and transport in the future, especially for the ITER relevant H-mode study such as P_{LH} estimation.

This work was supported by U.S. DOE Contracts DE-FG02-99ER54518, DE-AC02-09CH11466 and DE-AC05-00OR22725.

References:

- [1] Wagner F 2007 *Plasma Phys. Control. Fusion* **49** B1
- [2] Lee K C 2006 *Phys. Plasmas*, **13**, 062505, invited talk, APS DPP meeting 2006
- [3] Lee K C 2007 *Phys. Rev. Lett.* **99**, 065003.
- [4] Lee K C 2009 *Plasma Phys. Control. Fusion* **51** 065023.
- [5] Sabbagh S A, Kaye S M *et al* 2001 *Nucl. Fusion* **41**, 1601.
- [6] Lee K C, Domier C W *et al* 2004 *IEEE trans. Plasma Science*. **32**(4), 1721
- [7] Bell R E, Andre R, Kaye S M *et al* 2010 *Phys. Plasmas*, **17**, 082507